HHS Public Access

Author manuscript

Circulation. Author manuscript; available in PMC 2021 November 10.

Published in final edited form as:

Circulation. 2020 November 10; 142(19): 1848–1862. doi:10.1161/CIRCULATIONAHA.119.041433.

Single-cell RNA-seq Unveils Unique Transcriptomic Signatures of Organ-Specific Endothelial Cells

David T. Paik, PhD[1,2,3,*], **Lei Tian, PhD**[1,2,3,*], **Ian M. Williams, PhD**[1,3,4,*], **Siyeon Rhee, PhD**[4], **Hao Zhang, MD**[1,2,3], **Chun Liu, PhD**[1,2,3], **Ridhima Mishra, BS**[1], **Sean M. Wu, MD, PhD**[1,2,3], **Kristy Red-Horse, PhD**[1,3,4], **Joseph C. Wu, MD, PhD**[1,2,3]

[1]Stanford Cardiovascular Institute, Stanford University, Stanford, CA

[2]Department of Medicine, Division of Cardiology, Stanford University, Stanford, CA

[3]Institute for Stem Cell Biology and Regenerative Medicine, Stanford University, Stanford, CA

[4]Department of Biology, Stanford University, Stanford, CA

Abstract

Background: Endothelial cells (ECs) display considerable functional heterogeneity depending on the vessel and tissue in which they are located. While these functional differences are presumably imprinted in the transcriptome, the pathways and networks which sustain EC heterogeneity have not been fully delineated.

Methods: To investigate the transcriptomic basis of EC specificity, we analyzed single-cell RNA-sequencing (scRNA-seq) data from tissue-specific mouse ECs generated by the *Tabula Muris* consortium. We employed a number of bioinformatics tools to uncover markers and sources of EC heterogeneity from scRNA-seq data.

Results: We found a strong correlation between tissue-specific EC transcriptomic measurements generated by either scRNA-seq or bulk RNA-seq, thus validating the approach. Using a graph-based clustering algorithm, we found that certain tissue-specific ECs cluster strongly by tissue (e.g. liver, brain) whereas others (i.e. adipose, heart) have considerable transcriptomic overlap with ECs from other tissues. We identified novel markers of tissue-specific ECs and signaling pathways that may be involved in maintaining their identity. Sex was a considerable source of heterogeneity in the endothelial transcriptome and we discovered *Lars2* to be a gene that is highly enriched in ECs from male mice. In addition, we found that markers of heart and lung ECs in mice were conserved in human fetal heart and lung ECs. Finally, we identified potential angiocrine interactions between tissue-specific ECs and other cell types by analyzing ligand and receptor expression patterns.

Correspondence: Joseph C. Wu, MD, PhD, 265 Campus Drive, Room G1120B, Stanford, CA 94305-5454., Phone: (650) 736-2256, joewu@stanford.edu.

*Drs. Paik, Tian, and Williams contributed equally.

DISCLOSURES

Dr. Wu is a co-founder of Khloris Biosciences but has no competing interests, as the work presented here is completely independent. The other authors declare no competing interests.

Conclusions: In summary, we use scRNA-seq data generated by the *Tabula Muris* consortium to uncover transcriptional networks that maintain tissue-specific EC identity and to identify novel angiocrine and functional relationships between tissue-specific ECs.

Keywords

Single-cell RNA sequencing; endothelial cells; bioinformatics

INTRODUCTION

Endothelial cells (ECs) comprise the innermost lining of blood and lymphatic vessels. ECs play a critical role in tissue homeostasis by regulating blood flow, delivery of plasma-borne macromolecules, vessel formation, and adhesion of circulating blood cells[1]. As such, EC dysfunction can contribute to various disease mechanisms, including atherosclerosis and coronary artery disease[2], tumor vascularization[3], diabetic complications[4,5], and neurodegenerative disease[6].

While ECs are considered a single cell type, they exhibit considerable structural, phenotypic, and functional heterogeneity depending on the tissue in which they reside[7–10]. Furthermore, tissue-specific EC dysfunction can contribute to a number of different diseases. In the blood-brain barrier (BBB), for example, ECs are bound by tight junctions to maintain a highly selective, low permeability barrier. Endothelial dysfunction in the BBB can lead to Alzheimer's disease, epilepsy, and multiple sclerosis[11–13]. The cardiac endothelium plays a crucial role in promoting cardiomyocyte proliferation and maturation via paracrine signaling[14–16], whereas limited EC proliferative potential results in suboptimal repair of damaged heart tissue following ischemic injury[17]. Secretion of angiocrine factors from pulmonary ECs has been shown to improve lung alveolar regeneration[18], whereas angiocrine factors from liver sinusoidal ECs are critical in modulating hepatic regeneration[19]. Thus, understanding tissue-specific EC functionality is critical for treating a wide range of human diseases.

Given that ECs in different tissues have unique functions, it is reasonable to hypothesize that they also exhibit unique molecular signatures. Indeed, bulk microarray-based transcriptomic analyses of mouse[20,21] and human ECs[22], as well as bulk RNA sequencing of human fetal ECs[23], have demonstrated that ECs from different tissues have unique gene expression profiles. Bulk measurements, however, are unable to resolve transcriptomic heterogeneity that may exist between ECs from a given tissue. In addition to ECs from different vessel types (i.e., artery, vein), there may be as yet unidentified subpopulations of ECs within a tissue.

The recent advent of scRNA-seq addresses this limitation by allowing in-depth transcriptomic analysis of thousands of single cells at unprecedented resolution[24]. Recent studies have compiled single-cell transcriptomic[25,26] and epigenomic[27] data from all major mouse organs, including the endothelium[10]. Notably, the *Tabula Muris* investigators constructed an organism-wide transcriptomic profile using both plate-based and microdroplet-based scRNA-seq, resulting in an analysis of over 100,000 cells from 20 murine organs and tissues[26]. From this dataset, we extracted individual EC transcriptomes

from 12 organs to investigate the transcriptomic landscape of tissue-specific ECs. Using these transcripts, we determined markers, signaling pathways, and biological processes enriched in tissue-specific ECs. Importantly, we found that markers of murine tissue-specific ECs were conserved in human fetal ECs. Furthermore, we used an unsupervised clustering approach to identify novel EC subtypes. We also inferred potential paracrine EC-to-parenchymal cell interactions and sex differences in EC gene expression. Finally, we observed robust expression of *Lars2* in ECs of male mice, but its expression is low and variable in female ECs. In summary, we have harnessed scRNA-seq to delineate the transcriptomic heterogeneity that underlies tissue-specific EC function.

MATERIALS AND METHODS

Data availability

Analytic methods and the resulting data have been made available to other researchers for purposes of reproducing the results presented. Scripts used in the study are available on GitHub (https://github.com/Lei-Tian/multi-Organ-EC). Analyzed data in R objects are available on Figshare (https://figshare.com/articles/EC_TSNE_Robj/12170358).

scRNA-seq data pre-processing

We obtained SMART-Seq2 RNA-seq libraries of FACS-sorted single cells directly from the *Tabula Muris* database[26]. Seurat objects generated by the *Tabula Muris* investigators were downloaded from Figshare (https://figshare.com/account/home#/projects/27733). The majority of scRNA-seq data analysis was performed using the Seurat R package[28]. Annotations of each cell were downloaded from the *Tabula Muris* Github website (https://github.com/czbiohub/tabula-muris). ECs in all possible organs (12 in total) were extracted from the raw data. Cells with <500 detected genes and <50,000 confidentially mapped reads were excluded from downstream analysis. Raw counts were converted to log counts per million by log-normalization and subsequently scaled. The effects of confounding factors, including ribosomal RNA, total number of reads, and percentage of ERCC controls, were removed by linear regression. We then selected 5,203 highly variable genes (average expression >=0.1 and dispersion>=0.5) for downstream analysis.

Comparison of scRNA-seq and microarray data to determine global gene expression in tissue-specific ECs

Microarray-based transcriptomic measurements (Affymetrix GeneChip Mouse Gene 1.0 ST Array) of tissue-specific murine ECs were acquired previously by Rafii and colleagues[20] and accessed from GEO Omnibus (GSE47067). All microarray data were processed using the oligo and limma R packages[29,30]. Raw intensity values were background-corrected, normalized, and summarized using the robust multi-array average algorithm. Microarray data were compared to scRNA-seq data by averaging gene expression values across all replicate samples or cells. The top 10 differentially expressed genes (DEGs) in tissue-specific EC microarray data were identified using the empirical Bayesian method[28,31].

Dimensionality reduction and clustering

To initially reduce the dimensionality of the scRNA-seq dataset, we performed principal component (PC) analysis on highly variable genes. We chose the top 20 PCs for downstream analysis based on a resampling procedure[29] and the contribution of each PC to variance in the dataset. We then used the top 20 PCs to project cells onto 2-dimensional maps using both t-distributed Stochastic Neighbor Embedding (t-SNE) and Uniform Manifold Approximation and Projection (UMAP) algorithms[32]. Unsupervised clustering of single cells was performed using the FindClusters function in Seurat with the resolution parameter set at 0.8. Briefly, this function first finds the k-nearest neighbors for each cell in the PC space. Then, connections between cells are weighted based on their Jaccard similarity, or the number of *k*-nearest neighbors that they share, to construct a shared nearest neighbor graph[33]. Finally, densely connected cells are defined as clusters by optimizing modularity with the Louvain community detection method[34].

Cell-to-cell communication prediction analysis

To predict the intercellular communication between endothelial cells and functional cell types in each organ, we obtained ligand-receptor pairs compiled as previously described[35]. We defined a ligand or receptor as “expressed” in a particular cell type if 25% of the cells of that type had at least 1 read count for the gene encoding the ligand/receptor. To define networks of cell-to-cell communication, we linked any two cell types if the ligand was expressed in the former cell type and the receptor in the latter. Lines connecting cell populations are colored according to the population broadcasting the ligand and are connected to the population expressing the receptor. Networks were plotted using the igraph R package.

Immunofluorescence

Immunofluorescence was performed on 10 μm deparaffinized sections as previously described[36]. Six C57Bl/6 mice of 8–10 weeks of age (3 males and 3 females) were euthanized under approved Stanford University Administrative Panel on Laboratory Animal Care (APLAC) protocol #26923. All tissues were dissected and collected in PBS, then fixed overnight in 4% paraformaldehyde (PFA) at 4 °C. The following day, tissues were washed in PBS and PBT (PBS containing 0.1% Tween-20), dehydrated in an ascending methanol sequence, xylene treated, embedded in paraffin, and sectioned at 10 μm. Sections were subjected to antigen retrieval in Tris buffer pH 10.0 for 5 min, washed three times in 0.1% PBT, and incubated in blocking buffer (0.5% dried milk powder, 99.5% PBT) for 2 h at room temperature (RT). Primary antibodies were incubated in blocking buffer overnight at 4 °C with the following dilutions: Erg (Abcam, ab92513, 1:1,000), Endomucin (Santa Cruz, sc-65495, 1:250), and Lars2 (Proteintech, 17097–1-AP, 1:200). The next day, sections were washed three times with PBT and incubated for 1 h with corresponding secondary antibodies at 1:500 dilution in blocking buffer at RT. After three washes in PBS, DAPI (SigmaAldrich, 1:2,000) was added to counter-stain the nuclei. The sections were mounted using Prolong Gold Antifade Reagent (Invitrogen, P36934) and imaged using a Zeiss LSM 700 confocal microscope. All procedures were performed in accordance with the institutional guidelines of Stanford University APLAC.

Statistical methods for differential gene expression and pathway enrichment analysis

DEGs among tissues and clusters were detected by comparing ECs in each tissue or cluster against all other ECs using a Wilcoxon rank sum test. A gene was defined as a cluster or tissue's marker if it could be detected in ≥25% cells, and the log-fold change in its expression was ≥2 between cells of cluster X and all other cells (adjusted p-value < 0.05). For the analysis comparing male and female tissue-specific ECs, genes with an adjusted p-value < 0.05 were deemed DEGs. We then defined the top DEGs as the 5 DEGs with the highest average log-fold change compared to ECs from the opposite sex. All these analyses were performed in the Seurat package v2.3. Kyoto Encyclopedia of Genes and Genomes (KEGG) pathway enrichment analyses were performed with geneAnswers R package[37].

RESULTS

Identification of endothelial cells in single-cell transcriptomic data from 12 mouse organs

The *Tabula Muris* investigators performed scRNA-seq on 100,000+ cells in 20 major organs from 4 male and 3 female adult C57BL/6 mice[26]. As described in the original manuscript, cell type annotations were generated by identifying clusters within a given tissue that were defined by endothelial markers (Table I **in the** Supplement). Using these annotations, we extracted single EC transcriptome data in 12 organs (adipose tissue, aorta, brain, diaphragm, heart, kidney, liver, lung, mammary gland, pancreas, skeletal muscle, and trachea) with a sufficient number of ECs for downstream analyses (Fig. 1A,D & Fig. I **in the** Supplement). These cells have robust expression of endothelial genes, including *Pecam1*, *Cdh5*, *Tie1*, and *Egfl7* (Fig. II-A **in the** Supplement), with minimal expression of neuronal, kidney, and lung genes (Fig. II-B,E,F **in the** Supplement). Interestingly, some ECs do express hepatocyte (e.g., *Alb,* and *Ttr*) (Fig. II-C **in the** Supplement) and cardiomyocyte (e.g., *Tnnt2, Tnni3, and Nppa*) (Fig. II-D **in the** Supplement) markers, potentially reflecting the trans-differentiation potential of cardiac[34,35] and hepatic sinusoidal ECs[38]. In general, however, the majority of cells extracted from the *Tabula Muris* study show a uniformly strong expression of endothelial genes with little to no expression of parenchymal markers (Table II **in the** Supplement).

To determine whether scRNA-seq can capture tissue-specific EC transcriptomic signatures, we compared the *Tabula Muris* scRNA-seq EC data to a previously reported microarray dataset of ECs isolated from various mouse organs via intravital immunolabeling[20]. We observed strong correlations between scRNA-seq and microarray-based tissue-specific EC gene expression (Fig. III-A–F **in the** Supplement). Furthermore, the correlations of scRNA-seq and microarray-based gene expression measurements tend to be strongest when comparing ECs from the same tissue (Fig. III-G **in the** Supplement). Finally, we observed that when performing unsupervised hierarchical cluster analysis, tissue-specific ECs characterized by microarray clustered with *Tabula Muris* ECs from that same tissue (Fig. IV-G **in the** Supplement). In summary, the above analyses demonstrate that scRNA-seq can be used to effectively capture tissue-specific EC transcriptomic signatures from heterogeneous cell mixtures.

Heterogeneity and molecular signatures of tissue-specific endothelial cells

The *Tabula Muris* investigators observed 4 groups of transcriptomically distinct ECs when projecting cells from 20 mouse organs into 2-dimensional t-SNE space[26]. These groups include liver, lung, and brain ECs as well as a heterogeneous mixture of ECs from various tissues. To better resolve differences between tissue-specific ECs, we visualized ECs alone in 2-dimensional t-SNE space (Fig. 1B). Using this approach, we observed that ECs mostly segregate based on tissue of origin. ECs from some organs (e.g., brain, kidney, lung, and liver) appear to have unique transcriptomic identities, whereas ECs from other organs (e.g., adipose, heart, and aorta) show more overlap in gene expression as evidenced by UMAP (Fig. 1B,C). These findings suggest that different organs may possess varying levels of functional specialization from ECs.

To define markers of tissue-specific ECs, we identified transcripts enriched in ECs from each of the 12 organs using the non-parametric Wilcoxon rank-sum test. The top ten DEGs in ECs from each organ are shown in Fig. 2A, and the comprehensive list of DEGs in Table III **in the** Supplement. Bolded DEGs encode cell surface proteins that may be useful for targeted delivery of therapeutics to specific tissues. The most specialized DEG profiles were found in brain and pancreas ECs, which expressed mainly solute carrier transporters and digestive enzymes, respectively. To visualize the tissue-specificity of DEGs, we generated a heatmap displaying the expression of tissue-specific DEGs across all 12 organs. As seen in the t-SNE presentation (Fig. 1B), brain and liver ECs express unique sets of genes that are virtually undetected in ECs from other organs (Fig. 2B). Conversely, the DEGs characterizing heart, diaphragm, adipose tissue, skeletal muscle, and mammary gland ECs are less specific (Fig. 2B). We also found that, with the exception of liver ECs, the expression of tissue-specific EC DEGs identified previously by microarray[20] correlated well between microarray and scRNA-seq-based transcriptomic measurements (Fig. IV-A–F **in the** Supplement). These findings validate the utility of scRNA-seq for identifying the transcriptomic signature of tissue-specific ECs.

Using the identified organ-specific EC DEGs, we determined molecular pathways unique to organ-specific ECs by performing gene set enrichment analysis with the KEGG pathway database. Pathways associated with the greatest number of DEGs in ECs were visualized in chord plots for each of the 12 organs (Fig. 3A). Gene enrichment analysis identified both commonly shared and unique molecular and cellular pathways in ECs from different organs. Examples of unique pathways include osteoclast differentiation in adipose tissue ECs, ErbB signaling in brain ECs, axon guidance in cardiac ECs, and endocytosis in kidney ECs. Major developmental pathways known to play a critical role in endothelial homeostasis and function such as the Wnt, MAPK, cytokine-cytokine receptor interaction, and metabolism-associated pathways were commonly found in multiple organs. Interestingly, the majority of the genes associated with the common pathways in organ-specific ECs were unique (Table IV **&** Fig. V **in the** Supplement). For instance, Wnt signaling was found to be highly up-regulated in ECs from the brain, heart, liver, and lung, but the genes in organ-specific ECs contributing to Wnt signaling regulation were different. Namely, brain ECs show a higher expression of *Axin2*, *Fzd6*, and *Nkd1*, whereas cardiac ECs expressed *Ccnd1*, *Ctnnbip1*, and *Plcb4*, and liver ECs expressed *Apc*, *Ep300*, and *Lrp6*. Likewise, we identified unique DEGs

specific to ECs in each organ that are associated with MAPK signaling, cytokine-cytokine receptor interaction, and metabolic pathways.

Organ-specific angiocrine factors and ligand-receptor interaction

scRNA-seq of all cells collected from a given tissue enables gene expression comparison and analysis among individual cell types. A major known role of ECs in tissue homeostasis and function is mediated through the secretion of EC-specific paracrine factors called "angiocrine" factors[39]. We therefore sought to unveil unique angiocrine factors expressed by ECs in each organ. From the EC single-cell transcriptome, we identified potential ligand-receptor pairs between ECs and all sequenced parenchymal cell types in each of the 12 organs as previously described[35,40] (Fig. 3B, **left**). A comprehensive list of the identified ligand-receptor pairs is provided in Table V **in the** Supplement. This analysis revealed the existence of unique angiocrine ligand-receptor pairings between ECs and parenchymal cells in each organ. For example, *Efna1* expressed in brain ECs is known to bind to *Epha5* and *Pehb5* gene-coding receptors in neurons and oligodendrocyte precursor cells, whereas *Edn3* expression from ECs is projected to interact with *Ednra* in brain pericytes. Similarly, we depicted unique angiocrine and paracrine relationships in 8 major organs (Fig. 3B, **right**).

Unsupervised clustering analysis for identification of EC subpopulations

We utilized unsupervised clustering to identify novel subpopulations of ECs which may be independent of the tissue of origin. Specifically, we found 13 unique clusters using a graph-based clustering approach (Fig. 4A,B). We then determined the percentage (Fig. 4C) and the absolute numbers (Fig. VI-A **in the** Supplement) of ECs from each organ that comprised the 13 clusters, with the enriched gene list for each cluster provided in Table VI **in the** Supplement. Certain clusters show enrichment of ECs from a single organ, whereas other clusters are composed of ECs from various organs (Fig. 4C **&** Fig. VI-A **in the** Supplement). Conversely, we analyzed the proportion (Fig. 4D) and the absolute numbers (Fig. VI-B **in the** Supplement) of ECs in each organ that were assigned to the various clusters. Pathway enrichment analysis and cluster-specific DEGs allowed us to infer the biological identity of the unsupervised clusters (Fig. 4E–G **&** Fig. VII **in the** Supplement). For example, cluster 4 is a subpopulation of lung ECs that overexpresses transcripts involved in antigen processing and presentation, allograft rejection, and graft-versus-host disease (Fig. 4E), leading us to hypothesize this subpopulation may represent antigen-presenting ECs. Cluster 5 is comprised of ECs from a number of different organs that show enrichment of transcripts involved in toxoplasmosis, cytosolic DNA sensing, and MAPK signaling and therefore may be ECs responding to an infection (Fig. 4F). Cells in cluster 10 express genes in the stromal or smooth muscle cell lineage (Table VI **&** Fig. VII **in the** Supplement) and may represent ECs undergoing endothelial-to-mesenchymal transition. Finally, we found that ECs in cluster 9, a highly unique cluster in the transcriptome, had high expression of lymphatic markers such as *Prox1, Pdpn, Lyve1,* and *Flt4* (Fig. 4G **&** Fig. VI-C **in the** Supplement). In summary, we combined scRNA-seq with unsupervised clustering to identify EC subtypes that either reside within a single organ or in multiple organs.

Sex differences in the organ-specific endothelial cell transcriptome

As the *Tabula Muris* investigators analyzed both male and female mice, we probed for sex-dependent EC gene expression in brain, heart, lung, adipose tissue, aorta, and kidney (Fig. 5A **&** Fig. VIII-A–E **in the** Supplement). To ascertain the influence of sex on EC gene expression, we performed unsupervised clustering to determine whether ECs cluster by sex within a given organ (Fig. IX **&** Table VII **in the** Supplement). Some tissues (e.g., aorta, brain, lung) had subclusters of ECs that were comprised almost entirely of ECs from a single sex whereas other tissues (adipose tissue, heart, kidney) had a more even distribution of sex between subclusters. These findings suggest that there are subsets of ECs within certain tissues that are sex-specific. We also determined the top DEGs in male versus female organ-specific ECs (Fig. 5B **&** Fig. VIII-F–H **in the** Supplement) and used them to perform pathway enrichment analysis (Fig. 5C). Analysis of the overlap between DEGs identified in male versus female tissue-specific ECs indicated that the sex-dependency of DEGs varies amongst different tissues (Fig. X **in the** Supplement). Notably, we found *Lars2*, a non-sex-linked gene coding for leucyl-tRNA synthase 2, to be robustly and uniformly expressed in all male ECs, whereas its expression is low and highly variable in female ECs (Fig. 6A–B). While *Lars2* gene expression is relatively ubiquitous among various cell types (data not shown), LARS2 protein expression appeared largely specific to ECs in most organs (Fig. 6C). Similar to mRNA, LARS2 protein expression was enriched in male ECs, especially in the brain, heart ventricle, lung, and liver (Fig. 6C). Taken together, these findings indicate that sex is an important source of transcriptomic variation in tissue-specific ECs.

Correlation of mouse and human endothelial gene expression

In order to determine the relevance of our findings in murine ECs to human endothelial biology, we first compared the *Tabula Muris* dataset to bulk RNA-seq measurements made in ECs isolated from human fetal organs (e.g., heart, kidney, liver, and lung)[23]. We found that the correlation of adult murine and fetal human EC gene expression tends to be strongest when comparing ECs from the same organ (Fig. 7A). Furthermore, markers of tissue-specific ECs identified in mice were also enriched in their corresponding human tissue-specific ECs (Fig. 7B). These findings indicate that the transcriptomic manifestation of tissue-specificity in ECs is relatively well conserved between mice and humans. Finally, we checked the expression of the top 10 murine tissue-specific EC DEGs in human induced pluripotent stem cell (iPSC)- and human embryonic stem cell (ESC)-derived ECs and their progenitors generated previously by our group[40,41]. Progenitor iPSC-ECs showed an elevated expression of genes enriched in the aorta, adipose tissue, heart, and liver ECs (Fig. 7C, **middle panel**). Fully differentiated iPSC-ECs and ESC-ECs were most notably characterized by the expression of aorta, heart, liver, and mammary gland EC genes, while lacking expression of genes in the brain and pancreas ECs (Fig. 7C, **right panel**). Thus, the human pluripotent stem cell-derived ECs do not mimic ECs from any one particular tissue with respect to global gene expression, necessitating further development of methodologies to generate iPSC-ECs or ESC-ECs that possess organ-specific transcriptomic profiles to enable the most effective use in disease modeling or cell-based therapy applications.

DISCUSSION

The vasculature is present in all major organs, underpinning homeostasis and function throughout the body. It is versatile in its role to accommodate to the unique physiological function of each organ, such as in nutrient transport, endocrine signaling, waste disposal, and disease protection[7]. However, genes and molecular pathways that govern the organ-specific role of endothelial cells have not been clearly defined to date, primarily due to insufficient methodologies to investigate a single cell type from various tissues in parallel. Previous attempts to decipher functional and transcriptomic features of organ-specific endothelial cells were insightful but not comprehensive, suffering from a limited number of organs analyzed in parallel or from bulk analysis masking detection of small populations or lowly expressed genes[18,20].

The recent advances in scRNA-seq have resolved these limitations aided by the generation of transcriptomic and epigenetic atlases of major mammalian organs. Carmeliet and colleagues published a comprehensive atlas of single-cell transcriptome measurements made in murine ECs from various tissues[10]. With respect to tissue-specific EC markers, the overlap between studies was high for the brain, liver, and kidney, medium for the lung, and low for the heart. This finding highlights the necessity for comparing multiple studies to identify robust markers of tissue-specific ECs. These genes, especially those that code for membrane surface proteins, are promising targets for organ-specific delivery of small-molecule chemicals and DNA- or RNA-based therapeutics that possess greater target specificity with reduced risk of side effects.

As the *Tabula Muris* consortium utilized both male and female mice, we were able to look for sex differences in tissue-specific EC gene expression. We found that markers of tissue-specific ECs, enriched pathways, and endothelial subpopulations varied between male and female mice, especially in the brain, heart, and lung. This transcriptomic variation may, in part, drive known sex differences in endothelial biology[42] and cardiovascular disease risk[43]. Furthermore, when designing tissue-specific drug delivery strategies, it will be vital to ensure that EC membrane targets are robustly expressed in both males and females. We also discovered that *Lars2* gene coding for mitochondrial leucyl-tRNA synthetase was highly enriched in male compared to female ECs. Interestingly, *LAR2* variants are associated with multi-organ dysfunction with varying phenotypes between males and females[44]. Sex-differences in endothelial Lars2 expression may contribute to this phenotypic variation.

We also compared global gene expression between adult mouse and fetal human tissue-specific ECs as determined by single-cell and bulk RNA-seq, respectively. We found that, despite differences in the developmental stage, there was considerable overlap in gene expression between ECs from the same tissue. This suggests that, to a certain extent, the transcriptional manifestation of tissue-specificity in ECs is established during development. Multi-institutional collaborative efforts are currently underway to establish human cell atlases, including the Human Cell Atlas[45] and the Human BioMolecular Atlas Program[46], whose data when generated can similarly be analyzed to decipher tissue-specific transcriptomic features of human ECs. Specifically, the direct juxtaposition of mouse and human EC single-cell gene expression profiles will be critical in identifying similarities and

differences between tissue-specific ECs due to species, age, and sex. As there are differences between mice and humans with respect to vessel organization, morphology, and hemodynamics, we expect that this variation will be reflected at the transcriptomic level. The completed human scRNA-seq atlas will therefore be immensely valuable in addressing these questions.

Future studies will also delve into tissue-specific differences in arterial, venous, and lymphatic specification of blood vessels and identify transcriptomic and functional differences in larger vessels versus capillary ECs. The origin of vascular ECs has long been a topic of contentious debate, with a plethora of lineage tracing models and cell sorting performed to decipher the identities of stem/progenitor cell populations that give rise to the endothelium. Moreover, adult ECs innately possess a high level of plasticity, capable of undergoing endothelial-to-mesenchymal transition in various tissue types and disease states[47]. Further analysis of scRNA-seq datasets of ECs from all organs during embryonic development or in association with aging and disease conditions will provide profound and novel information in addressing these questions[48].

Supplementary Material

Refer to Web version on PubMed Central for supplementary material.

Acknowledgments

SOURCES OF FUNDING

We are grateful for funding support from the National Institutes of Health (NIH) K99 HL150216 and Stanford Cardiovascular Institute Seed Grant (D.T.P.); American Heart Association (AHA) Postdoctoral Fellowship 20POST35210924 (L.T.); NIH T32 HL098049 (I.M.W.); AHA Undergraduate Summer Research Program (R.M.); and NIH R01 HL145676, R01 HL113006, R01 HL123968, R01 HL141851, and AHA 17MERIT33610009 (J.C.W.).

Non-standard Abbreviations and Acronyms

EC	Endothelial cell
DEG	Differentially expressed gene
Lars2	Leucyl-tRNA synthase 2
PC	Principal component
scRNA-seq	Single-cell RNA sequencing
tSNE	t-distributed stochastic neighbor embedding
UMAP	Uniform manifold approximation and projection

REFERENCES

1. Cines DB, Pollak ES, Buck CA, Loscalzo J, Zimmerman GA, McEver RP, Pober JS, Wick TM, Konkle BA, Schwartz BS, Barnathan ES, McCrae KR, Hug BA, Schmidt AM, Stern DM.

Endothelial cells in physiology and in the pathophysiology of vascular disorders. Blood. 1998;91:3527–3561. [PubMed: 9572988]

2. Vanhoutte PM, Shimokawa H, Feletou M, Tang EHC. Endothelial dysfunction and vascular disease - a 30th anniversary update. Acta Physiol Oxf Engl. 2017;219:22–96.
3. Dudley AC. Tumor endothelial cells. Cold Spring Harb Perspect Med. 2012;2:a006536. [PubMed: 22393533]
4. Tabit CE, Chung WB, Hamburg NM, Vita JA. Endothelial dysfunction in diabetes mellitus: molecular mechanisms and clinical implications. Rev Endocr Metab Disord. 2010;11:61–74. [PubMed: 20186491]
5. Rohlenova K, Goveia J, García-Caballero M, Subramanian A, Kalucka J, Treps L, Falkenberg KD, de Rooij LPMH, Zheng Y, Lin L, et al. Single-cell RNA sequencing maps endothelial metabolic plasticity in pathological angiogenesis. Cell Metab 2020;31:862–877.e14. [PubMed: 32268117]
6. Koizumi K, Wang G, Park L. Endothelial dysfunction and amyloid-β-induced neurovascular alterations. Cell Mol Neurobiol. 2016;36:155–165. [PubMed: 26328781]
7. Aird WC. Phenotypic heterogeneity of the endothelium: I. Structure, function, and mechanisms. Circ Res. 2007;100:158–173. [PubMed: 17272818]
8. Augustin HG, Koh GY. Organotypic vasculature: From descriptive heterogeneity to functional pathophysiology. Science. 2017;357:eaal2379. [PubMed: 28775214]
9. Gomez-Salinero JM, Rafii S. Endothelial cell adaptation in regeneration. Science. 2018;362:1116–1117. [PubMed: 30523098]
10. Kalucka J, de Rooij LPMH, Goveia J, Rohlenova K, Dumas SJ, Meta E, Conchinha NV, Taverna F, Teuwen L-A, Veys K, et al. Single-cell transcriptome atlas of murine endothelial cells. Cell. 2020;180:764–779.e20. [PubMed: 32059779]
11. Fabene PF, Navarro Mora G, Martinello M, Rossi B, Merigo F, Ottoboni L, Bach S, Angiari S, Benati D, Chakir A, et al. A role for leukocyte-endothelial adhesion mechanisms in epilepsy. Nat Med. 2008;14:1377–1383. [PubMed: 19029985]
12. Minagar A, Maghzi AH, McGee JC, Alexander JS. Emerging roles of endothelial cells in multiple sclerosis pathophysiology and therapy. Neurol Res. 2012;34:738–745. [PubMed: 22828184]
13. Erickson MA, Banks WA. Blood-brain barrier dysfunction as a cause and consequence of Alzheimer's disease. J Cereb Blood Flow Metab Off J Int Soc Cereb Blood Flow Metab. 2013;33:1500–1513.
14. Hsieh PCH, Davis ME, Lisowski LK, Lee RT. Endothelial-cardiomyocyte interactions in cardiac development and repair. Annu Rev Physiol. 2006;68:51–66. [PubMed: 16460266]
15. Tian Y, Morrisey EE. Importance of myocyte-nonmyocyte interactions in cardiac development and disease. Circ Res. 2012;110:1023–1034. [PubMed: 22461366]
16. Odiete O, Hill MF, Sawyer DB. Neuregulin in cardiovascular development and disease. Circ Res. 2012;111:1376–1385. [PubMed: 23104879]
17. Paik DT, Rai M, Ryzhov S, Sanders LN, Aisagbonhi O, Funke MJ, Feoktistov I, Hatzopoulos AK. Wnt10b gain-of-function improves cardiac repair by arteriole formation and attenuation of fibrosis. Circ Res. 2015;117:804–816. [PubMed: 26338900]
18. Ding B-S, Nolan DJ, Guo P, Babazadeh AO, Cao Z, Rosenwaks Z, Crystal RG, Simons M, Sato TN, Worgall S, et al. Endothelial-derived angiocrine signals induce and sustain regenerative lung alveolarization. Cell. 2011;147:539–553. [PubMed: 22036563]
19. Ding B-S, Nolan DJ, Butler JM, James D, Babazadeh AO, Rosenwaks Z, Mittal V, Kobayashi H, Shido K, Lyden D, et al. Inductive angiocrine signals from sinusoidal endothelium are required for liver regeneration. Nature. 2010;468:310–315. [PubMed: 21068842]
20. Nolan DJ, Ginsberg M, Israely E, Palikuqi B, Poulos MG, James D, Ding B-S, Schachterle W, Liu Y, Rosenwaks Z, et al. Molecular signatures of tissue-specific microvascular endothelial cell heterogeneity in organ maintenance and regeneration. Dev Cell. 2013;26:204–219. [PubMed: 23871589]
21. Lother A, Bergemann S, Deng L, Moser M, Bode C, Hein L. Cardiac endothelial cell transcriptome. Arterioscler Thromb Vasc Biol. 2018;38:566–574. [PubMed: 29301788]

22. Chi J-T, Chang HY, Haraldsen G, Jahnsen FL, Troyanskaya OG, Chang DS, Wang Z, Rockson SG, van de Rijn M, Botstein D, et al. Endothelial cell diversity revealed by global expression profiling. Proc Natl Acad Sci U S A. 2003;100:10623–10628. [PubMed: 12963823]
23. Marcu R, Choi YJ, Xue J, Fortin CL, Wang Y, Nagao RJ, Xu J, MacDonald JW, Bammler TK, Murry CE, et al. Human organ-specific endothelial cell heterogeneity. iScience. 2018;4:20–35. [PubMed: 30240741]
24. Paik DT, Cho S, Tian L, Chang HY, Wu JC. Single-cell RNA sequencing in cardiovascular development, disease and medicine. Nat Rev Cardiol. 2020;17:457–473. [PubMed: 32231331]
25. Han X, Wang R, Zhou Y, Fei L, Sun H, Lai S, Saadatpour A, Zhou Z, Chen H, Ye F, et al. Mapping the mouse cell atlas by microwell-seq. Cell. 2018;172:1091–1107.e17. [PubMed: 29474909]
26. Tabula Muris Consortium, Overall coordination, Logistical coordination, Organ collection and processing, Library preparation and sequencing, Computational data analysis, Cell type annotation, Writing group, Supplemental text writing group, Principal investigators. Single-cell transcriptomics of 20 mouse organs creates a Tabula Muris. Nature. 2018;562:367–372. [PubMed: 30283141]
27. Cusanovich DA, Hill AJ, Aghamirzaie D, Daza RM, Pliner HA, Berletch JB, Filippova GN, Huang X, Christiansen L, DeWitt WS, et al. A Single-cell atlas of in vivo mammalian chromatin accessibility. Cell. 2018;174:1309–1324.e18. [PubMed: 30078704]
28. Stuart T, Butler A, Hoffman P, Hafemeister C, Papalexi E, Mauck WM, Hao Y, Stoeckius M, Smibert P, Satija R. Comprehensive integration of single-cell data. Cell. 2019;177:1888–1902.e21. [PubMed: 31178118]
29. Carvalho BS, Irizarry RA. A framework for oligonucleotide microarray preprocessing. Bioinforma Oxf Engl. 2010;26:2363–2367.
30. Ritchie ME, Phipson B, Wu D, Hu Y, Law CW, Shi W, Smyth GK. limma powers differential expression analyses for RNA-sequencing and microarray studies. Nucleic Acids Res. 2015;43:e47. [PubMed: 25605792]
31. Smyth GK. Linear models and empirical bayes methods for assessing differential expression in microarray experiments. Stat Appl Genet Mol Biol. 2004;3:Article3.
32. Becht E, McInnes L, Healy J, Dutertre C-A, Kwok IWH, Ng LG, Ginhoux F, Newell EW. Dimensionality reduction for visualizing single-cell data using UMAP. Nat Biotechnol. 2019;37:38–44.
33. Levine JH, Simonds EF, Bendall SC, Davis KL, Amir ED, Tadmor MD, Litvin O, Fienberg HG, Jager A, Zunder ER, et al. Data-driven phenotypic dissection of AML reveals progenitor-like cells that correlate with prognosis. Cell. 2015;162:184–197. [PubMed: 26095251]
34. Blondel VD, Guillaume J-L, Lambiotte R, Lefebvre E. Fast unfolding of communities in large networks. J Stat Mech Theory Exp. 2008;2008:P10008.
35. Ramilowski JA, Goldberg T, Harshbarger J, Kloppmann E, Kloppman E, Lizio M, Satagopam VP, Itoh M, Kawaji H, Carninci P, et al. A draft network of ligand-receptor-mediated multicellular signalling in human. Nat Commun. 2015;6:7866. [PubMed: 26198319]
36. Rhee S, Chung JI, King DA, D'amato G, Paik DT, Duan A, Chang A, Nagelberg D, Sharma B, Jeong Y, et al. Endothelial deletion of Ino80 disrupts coronary angiogenesis and causes congenital heart disease. Nat Commun. 2018;9:368. [PubMed: 29371594]
37. Feng G, Du P, Krett NL, Tessel M, Rosen S, Kibbe WA, Lin SM. A collection of bioconductor methods to visualize gene-list annotations. BMC Res Notes. 2010;3:10. [PubMed: 20180973]
38. Tan Z, Chen K, Shao Y, Gao L, Wang Y, Xu J, Jin Y, Hu X, Wang Y. Lineage tracing reveals conversion of liver sinusoidal endothelial cells into hepatocytes. Dev Growth Differ. 2016;58:620–631. [PubMed: 27506985]
39. Rafii S, Butler JM, Ding B-S. Angiocrine functions of organ-specific endothelial cells. Nature. 2016;529:316–325. [PubMed: 26791722]
40. Paik DT, Tian L, Lee J, Sayed N, Chen IY, Rhee S, Rhee J-W, Kim Y, Wirka RC, Buikema JW, et al. Large-scale single-cell RNA-seq reveals molecular signatures of heterogeneous populations of human induced pluripotent stem cell-derived endothelial cells. Circ Res. 2018;123:443–450. [PubMed: 29986945]

41. Zhao M-T, Chen H, Liu Q, Shao N-Y, Sayed N, Wo H-T, Zhang JZ, Ong S-G, Liu C, Kim Y, et al. Molecular and functional resemblance of differentiated cells derived from isogenic human iPSCs and SCNT-derived ESCs. Proc Natl Acad Sci U S A. 2017;114:E11111–E11120. [PubMed: 29203658]

42. Stanhewicz AE, Wenner MM, Stachenfeld NS. Sex differences in endothelial function important to vascular health and overall cardiovascular disease risk across the lifespan. Am J Physiol Heart Circ Physiol. 2018;315:H1569–H1588. [PubMed: 30216121]

43. Mosca L, Barrett-Connor E, Wenger NK. Sex/gender differences in cardiovascular disease prevention: what a difference a decade makes. Circulation. 2011;124:2145–2154. [PubMed: 22064958]

44. Riley LG, Rudinger-Thirion J, Frugier M, Wilson M, Luig M, Alahakoon TI, Nixon CY, Kirk EP, Roscioli T, Lunke S, et al. The expanding LARS2 phenotypic spectrum: HLASA, Perrault syndrome with leukodystrophy, and mitochondrial myopathy. Hum Mutat. 2020;41:1425–1434. [PubMed: 32442335]

45. Regev A, Teichmann SA, Lander ES, Amit I, Benoist C, Birney E, Bodenmiller B, Campbell P, Carninci P, Clatworthy M, et al. The Human Cell Atlas. eLife. 2017;6:e27041. [PubMed: 29206104]

46. Consortium HuBMAP. The human body at cellular resolution: the NIH Human Biomolecular Atlas Program. Nature. 2019;574:187–192. [PubMed: 31597973]

47. Dejana E, Hirschi KK, Simons M. The molecular basis of endothelial cell plasticity. Nat Commun. 2017;8:14361. [PubMed: 28181491]

48. Tabula Muris Consortium. A single-cell transcriptomic atlas characterizes ageing tissues in the mouse. Nature. 2020;583:590–595. [PubMed: 32669714]

CLINICAL PERSPECTIVE

What is new?

- We identified signature markers, transcriptional networks, angiocrine signaling pathways, and cellular subpopulations enriched in endothelial cells from various mouse tissues.
- We uncovered sex differences in tissue-specific endothelial gene expression.
- We found that markers of tissue-specific endothelial cells are conserved between mice and humans.

What are the clinical implications?

- Novel endothelial cell membrane surface markers that can be targeted for tissue-specific drug delivery.
- Differentially expressed genes between male and female tissue-specific endothelial cells can be exploited to develop sex-specific cardiovascular disease models and treatments.

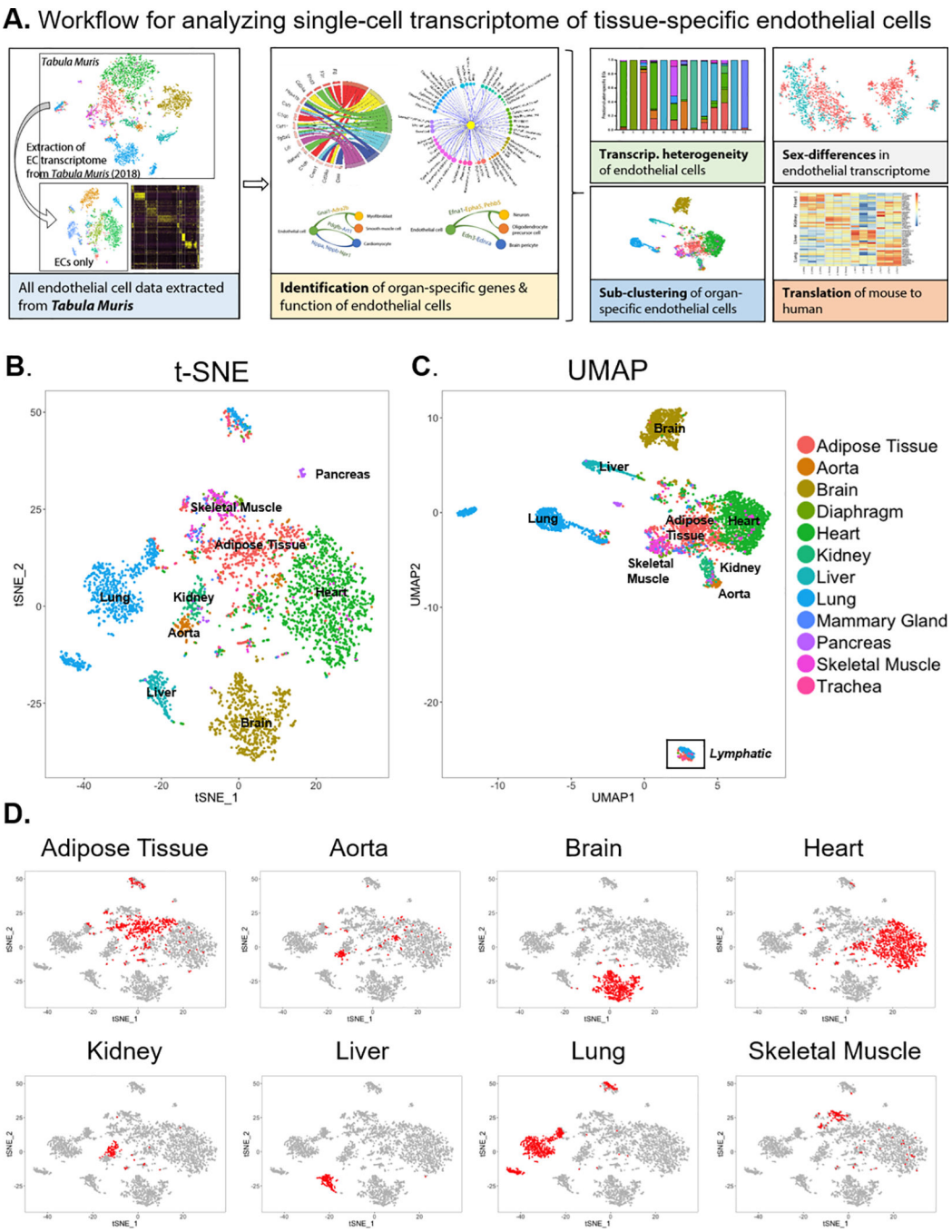

Figure 1. Single-cell transcriptome of endothelial cells in 12 major organs extracted from the *Tabula Muris* dataset.

(A) Experimental workflow for analyzing single-cell transcriptomes of tissue-specific endothelial cells (ECs). Projection of ECs onto **(B)** t-distributed Stochastic Neighbor Embedding (t-SNE) and **(C)** Uniform Manifold Approximation and Projection (UMAP) plots. ECs are color-coded by their tissue of origin. **(D)** Location of organ-specific ECs for 8 major individual organs on the t-SNE plot.

A.

Adipose Tissue	Aorta	Brain
Car3	***Tmem26***	***Slco1c1***
Csf2rb	*Igfbp5*	***Slco1a4***
Angptl4	*Il33*	***Slc22a8***
Egr2	*Dram1*	***Mfsd2a***
Gpr160	*Ehd3*	***Slc38a3***
Ifi27l2a	*Esm1*	*Spock2*
Lmo1	*Rarb*	*Foxf2*
Cldn15	*Fkbp5*	*Edn3*
Hexim1	***Enpep***	***Stra6***
Lgals1	*Cdc14a*	***Slc38a5***

Diaphragm	Heart	Kidney
Gm12216	*Wt1*	*Dram1*
Adamts4	***Slc28a2***	*Dkk2*
Sphk1	*Eepd1*	*Esm1*
Prkcc	***Kcna5***	*Igfbp5*
Rnd1	*Car8*	*Pbx1*
Nup210l	*Fbln1*	***Boc***
D730005E14Rik	*Meox2*	*Igfbp3*
Pde12	***Rftn1***	*Irx3*
Fosl2	*Lamb1*	*Tnfaip2*
Arid5a	***Myadm***	***Ptpru***

Liver	Lung	Mammary Gland
Dnase1l3	*Grtp1*	*Csf3*
Clec4g	***Adrb1***	*Il6*
Fcgr2b	***Scn7a***	*Fosl1*
Stab2	***Tmem100***	***Emp1***
Oit3	*Hpgd*	*Myc*
Bmp2	*Foxf1a*	*Efhd1*
Aass	*Nckap5*	*Adamts4*
Mrc1	*Rasgef1a*	*Stx11*
Plxnc1	*Fendrr*	*Mnda*
Wnt2	*Prx*	*Hbegf*

Pancreas	Skeletal Muscle	Trachea
Cela2a	*Cxcl10*	***Selp***
Prss2	*Cxcl2*	*Rgs16*
Cela1	*Adamts4*	***Itgb4***
Try4	*Rnd1*	*Col13a1*
Pnlip	*Cxcl1*	*Stc1*
Ctrb1	*Il6*	*Psd*
Cela3b	*Sphk1*	*Nr4a2*
Cel	***Icam1***	*Bhlhe40*
Clps	*Pfkfb3*	*Prkcc*
Cpa1	*Tubb6*	*Dusp2*

B.

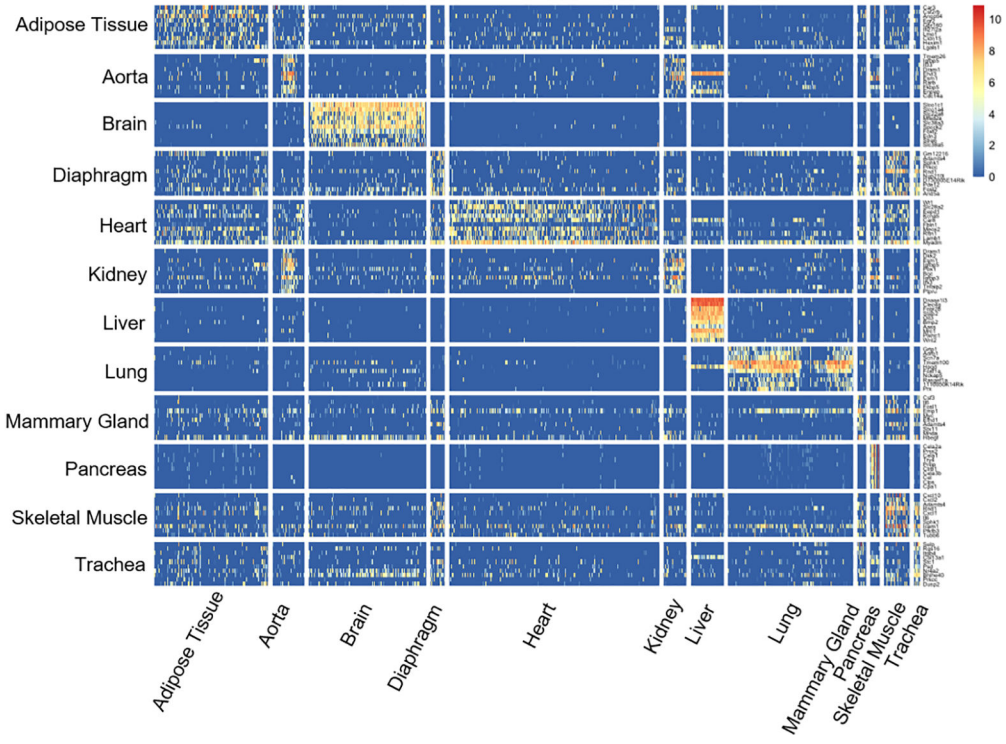

Figure 2. Identification of differentially expressed genes in organ-specific endothelial cells.

(A) Top ten differentially expressed genes in ECs of each of the 12 organs as determined by Wilcoxon rank-sum test. Blue indicate genes that encode for cell surface proteins. **(B)** Heatmap depicting expression levels of the top ten organ-specific differentially expressed genes (DEGs) in ECs from different organs. Rows indicate each gene and columns indicate single cells.

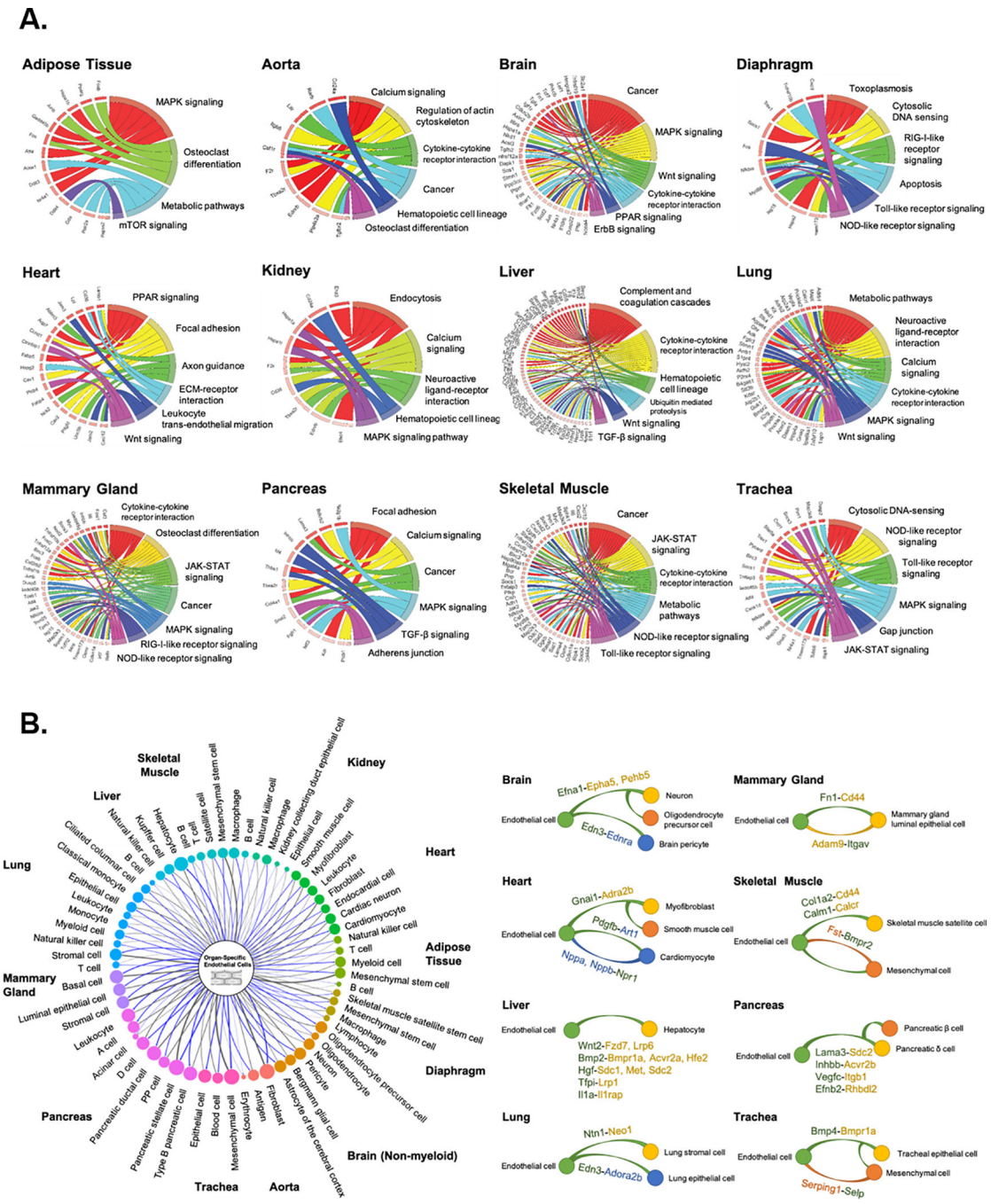

Figure 3. Pathway enrichment and angiocrine relationship prediction analyses.

(A) Kyoto Encyclopedia of Genes and Genomes (KEGG) pathway enrichment analysis of DEGs of tissue-specific ECs reveals unique organ-specific EC genes in signaling and cellular pathways, shown in chord plots. **(B)** Predicted angiocrine relationships between organ-specific ECs (left, center) and parenchymal cells (left, perimeter) from the same organ. Relationships are determined by expression of a secreted ligand in one cell type and its corresponding receptor in another. The thickness of connecting lines and size of bubbles indicate the number of ligand-receptor pairs. Representative organ-specific ligand-to-

receptor pairs are shown for 8 major organs (right). In the representative pairs shown, the ligand is written as the former and the receptor as the latter followed by a dash. Cell type which expresses each gene is noted by the color. Green represents endothelial cells and yellow, orange, and blue represent parenchymal cell types in each organ as shown.

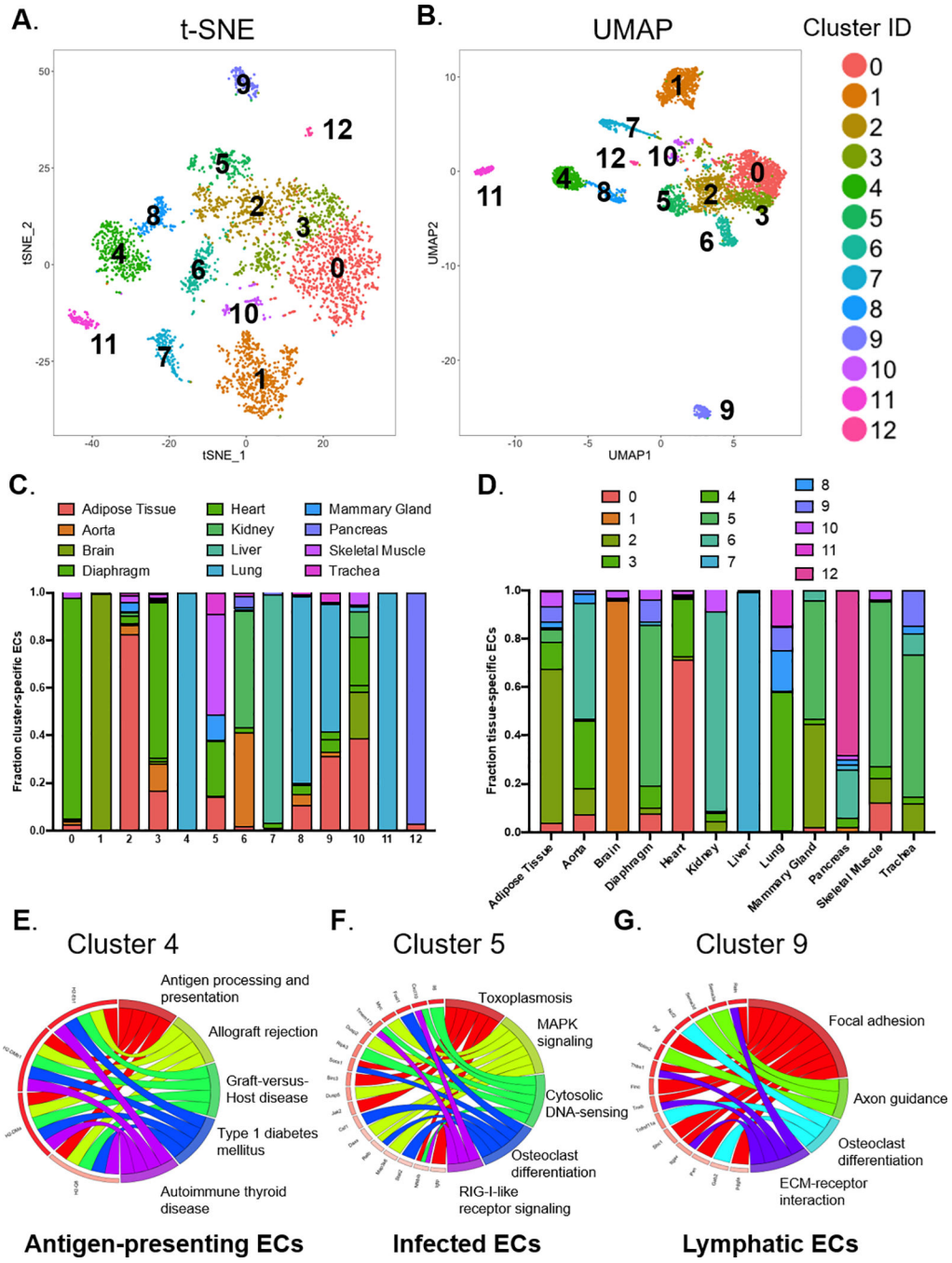

Figure 4. Unsupervised clustering to reveal subpopulations of ECs.

13 individual clusters (numbered 0 to 12) identified from a graph-based unsupervised clustering approach are shown in **(A)** t-SNE and **(B)** UMAP plots. **(C)** Proportion of ECs originating from different organs in each of the unsupervised clusters. **(D)** Proportion of ECs from unsupervised clusters in each of the 12 major organs. Based on KEGG pathway enrichment analysis of DEGs for each cluster, **(E)** “Cluster 4” represents antigen-presenting ECs, **(F)** “Cluster 5” represents infected ECs, and **(G)** “Cluster 9” represents lymphatic ECs.

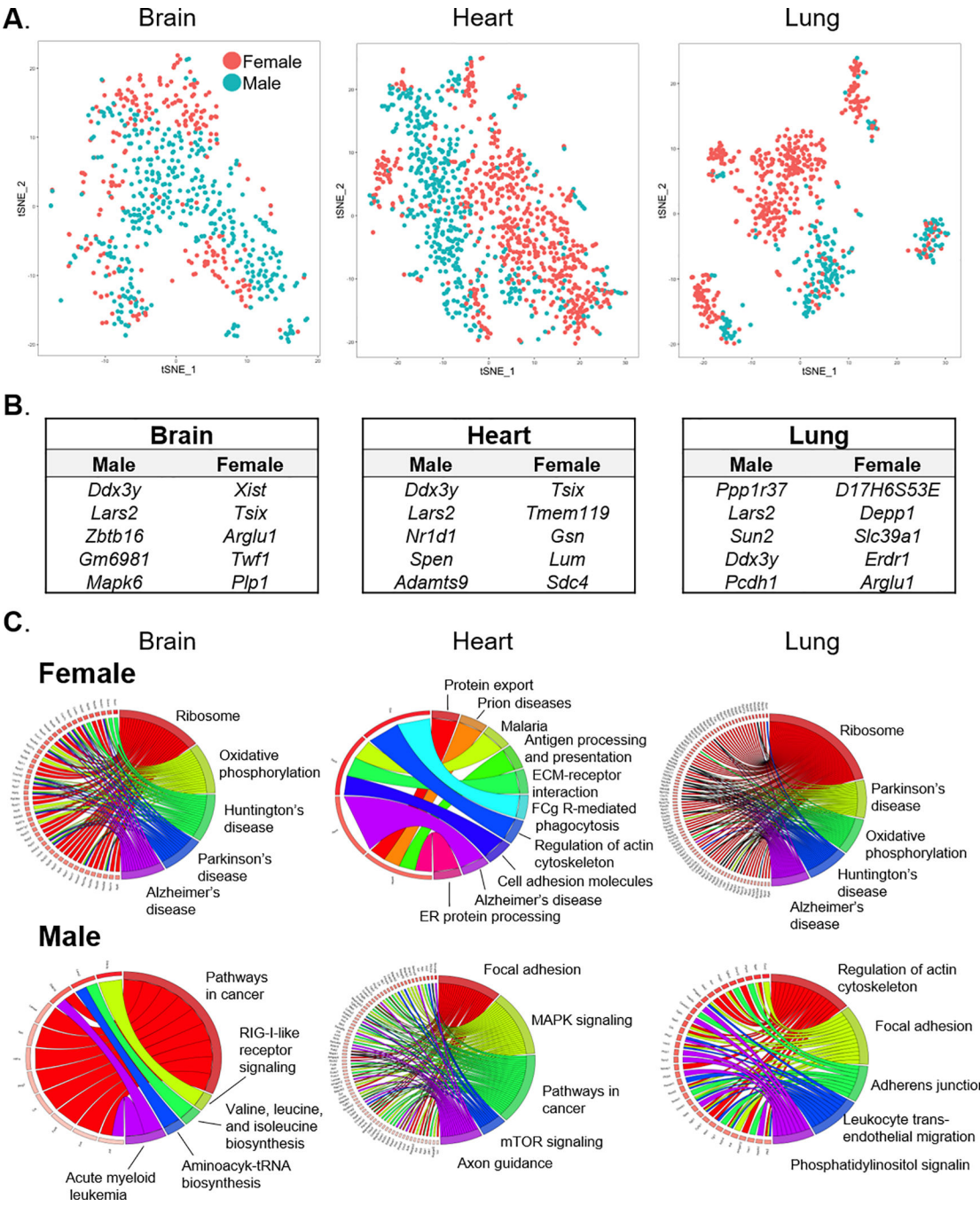

Figure 5. Sex differences in tissue-specific EC gene expression.

(A) Projections of ECs from brain, heart, and lung onto t-SNE maps color-coded by sex. **(B)** List of genes differentially expressed between male and female ECs in each organ. **(C)** KEGG pathway enrichment analysis of sex- and organ-specific DEGs show correlation of sex-dependent genes in ECs with organ-specific disease and/or cellular pathways.

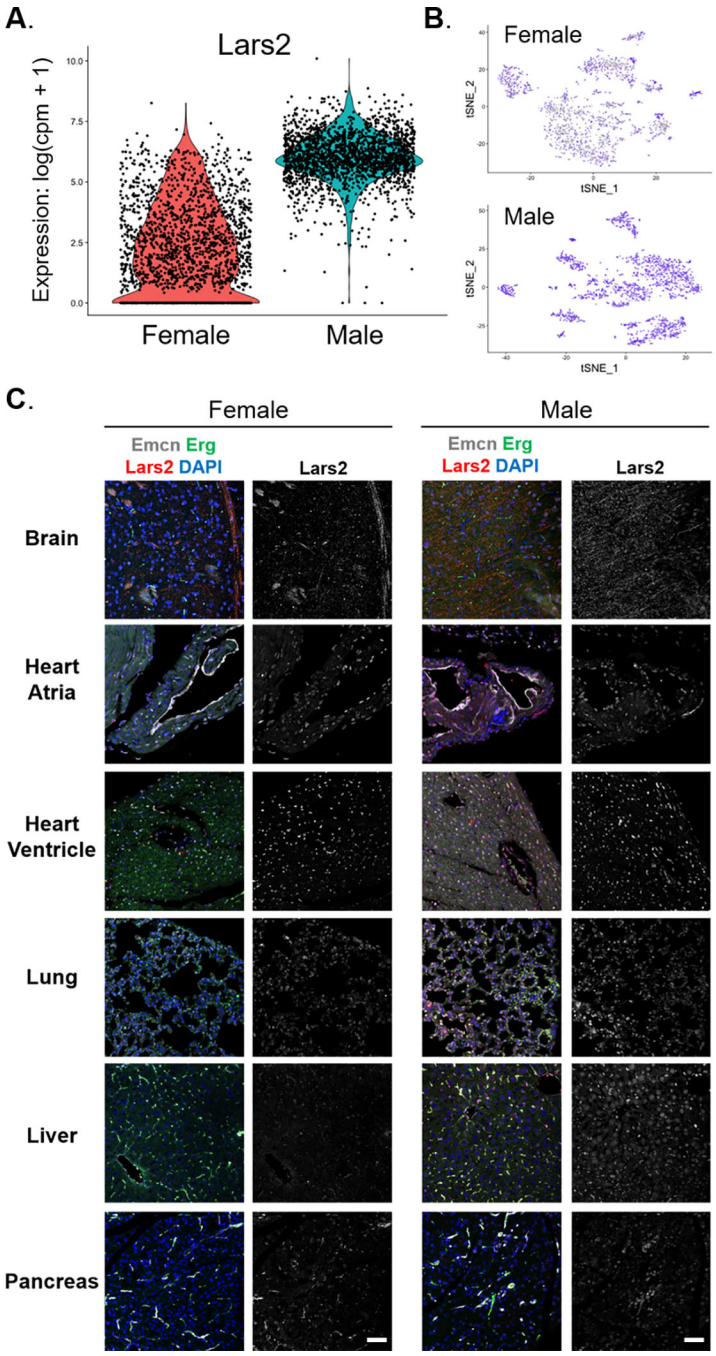

Figure 6. Lars2 expression is unique to male endothelial cells.

Endothelial cells from male mice exhibit higher expression of *Lars2* gene than females. **(A)** Violin plot shows the expression level of Lars2 in endothelial cells from male and female mice. Expression value is shown as log(counts per million + 1). **(B)** Expression level of Lars2 shown on t-SNE projection of endothelial cells from female and male mice. Blue and grey indicate cells with high and low expression of Lars2, respectively. **(C)** Immunofluorescent staining of various adult mouse organs from male and female mice shows enriched expression of LARS2 protein (red, left panel) in male brain, heart ventricle,

lung, and liver tissues, which co-localizes with the endothelial nuclear marker Erg (green, left panel). Scale bar, 50 μm.

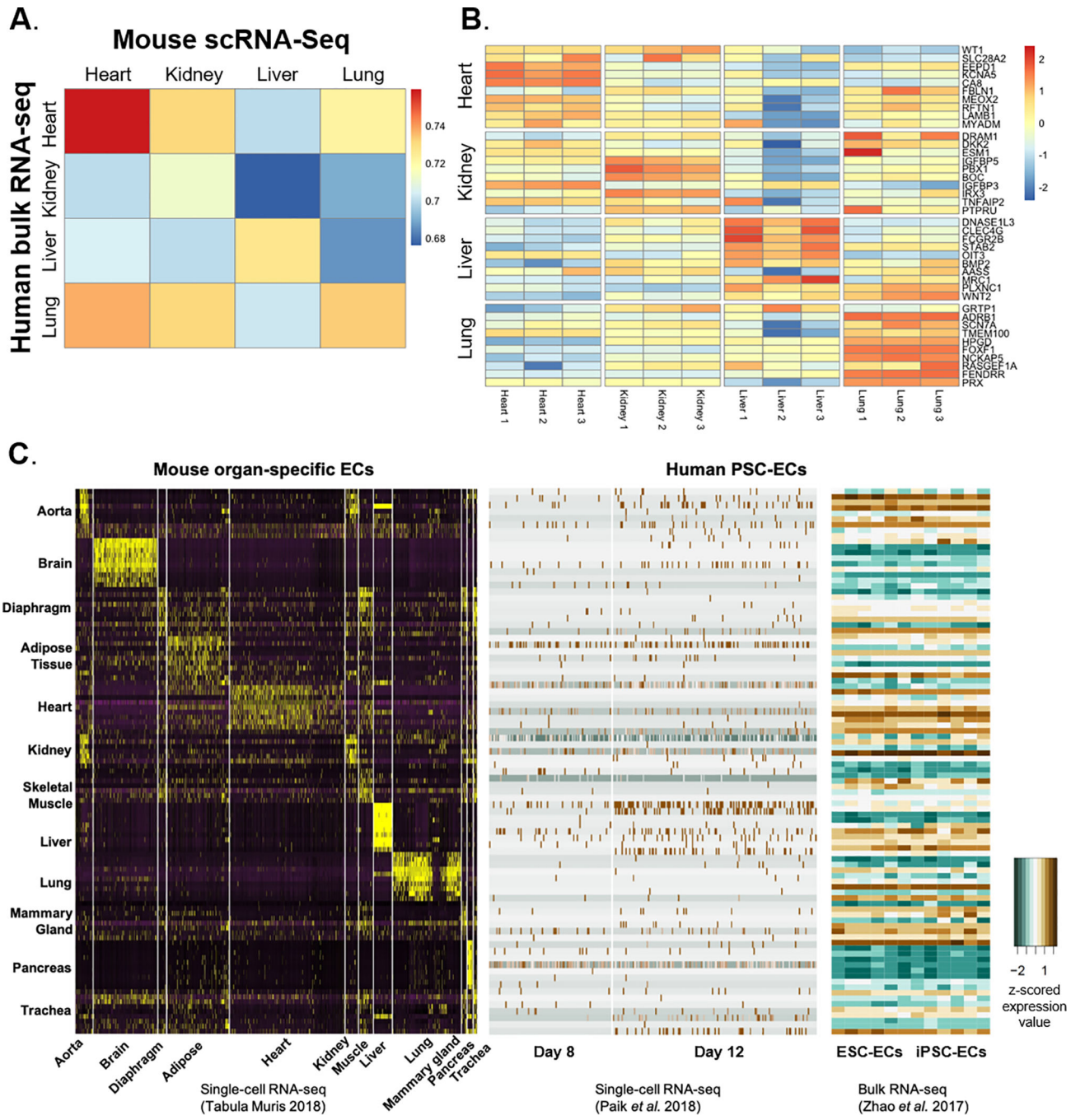

Figure 7. Mouse-to-human translation of organ-specific EC transcriptome.

(A) Correlation between murine EC gene expression with the corresponding human organ obtained from a previously published dataset (Marcu et al., 2018)[23]. Heatmap shows Spearman's rank correlation coefficients. **(B)** Expression values (log counts per million) of murine organ-specific EC DEGs in the corresponding human organ-specific ECs (Marcu et al., 2018)[23]. **(C)** z-scored expression value of DEGs in organ-specific ECs from mice are assessed in human induced pluripotent stem cell-derived EC transcriptome obtained from

the published single-cell (Paik et al., 2018)[40] and bulk (Zhao et al., 2017)[41] RNA-seq datasets.